VALIDATION OF ACTIVATION CALCULATIONS WITH MCNPX WITH SAMPLES FROM A COPPER BEAM DUMP

M. Wohlmuther[1], D. Schumann[1], P. Kubik[2], H.-A. Synal[2], V. Alfimov[3], G. Korschinek[4] , G. Rugel[4], T. Faestermann[4], M. Poutivtsev[4]

[1]*Paul Scherrer Institut, CH-5232 Villigen PSI, Switzerland, michael.wohlmuther@psi.ch*
[2] *Paul Scherrer Institut, c/o Institute of Particle Physics, ETH Zurich, 8093 Zurich, Switzerland*
[3] *Institute of Particle Physics, ETH Zurich, 8093 Zurich, Switzerland*
[4] *Physik-Department, Technische Universität München, D-85748 Garching, Germany*

All particles that are accelerated in an accelerator facility are lost somewhere. Some of those loss points are intentionally designed, such as collimators, slits, beam dumps and targets. The particles will interact with surrounding matter, initiate particle cascades and thereby activate the materials in the environment of the loss points. The biomedical area (BMA) beam dump is such a loss point which was irradiated for 12 years with 590 MeV protons in the so called biomedical area at PSI. After dismantling the copper beam dump was cut into pieces. Samples from the beam dump were taken at different depths and radial positions. Several radionuclides of interest for a final repository as well as nuclides relevant for gamma dose considerations such as ^{60}Co, ^{44}Ti, ^{36}Cl, ^{53}Mn, ^{55}Fe, ^{63}Ni, ^{26}Al and ^{108m}Ag have been investigated. In this paper we will present a comparison of calculated and measured nuclide contents of the BMA beam dump.

I. INTRODUCTION

The activation of accelerator components due to beam losses can be modeled using Monte Carlo particle transport codes like MCNPX[1] or FLUKA[2] in conjunction with buildup and decay codes (sometimes called transmutation or inventory codes). In recent MCNPX versions the buildup and decay code feature has been implemented for criticality problems, but not yet for fixed source problems, while FLUKA has a built-in buildup and decay code. Recently a collaboration of four institutes - Oak Ridge National Laboratory (ORNL), Argonne National Laboratory (ANL), Los Alamos National Laboratory (LANL) and the Paul Scherrer Institut (PSI) - has developed a Perl script[3] to automate the calculation of nuclide inventories for fixed source problems using the particle transport codes MCNP[4] and MCNPX together with the buildup and decay codes CINDER'90[5], FISPACT[6] and ORIHET-3[7].

In order to evaluate the predictive power of the models that are used in particle transport codes dedicated benchmark experiments have been performed[8-10] by other groups.

At the Paul Scherrer Institut (PSI) effort is put into the development of calculation methods for the activation of accelerator components, as for the disposal of dismantled accelerator components a characterization with respect to the nuclide inventory is mandatory. In this context long-lived isotopes are of interest due to requirements for the final repository. These calculations have to be constantly validated. Hence the comparison of theoretical prediction with experimental investigation of samples from representative dismantled accelerator components serves as a continuous quality assurance program. One of the "samples" is the beam dump of the so called PIOTRON, a facility to treat cancer patients with pions, operated at PSI from 1980 until 1992. It was then decided to use the copper beam dump to investigate the predictive power of the methods to calculate activation of accelerator components. The main focus was put on radionuclides which are rather long-lived. Besides gamma dose relevant nuclides such as ^{60}Co the isotope production of ^{26}Al, ^{36}Cl, ^{44}Ti, ^{53}Mn, ^{55}Fe, ^{63}Ni and ^{108m}Ag was investigated. In order to measure activities of these radionuclides some had to be separated chemically from the bulk material. Subsequently their activity was measured with accelerator mass spectrometry (AMS), liquid scintillation counting (LSC) or gamma spectroscopy depending on the decay mode.

In the next section details about the beam dump will be given, followed by the description of the calculation method. Finally, a comparison of measured and calculated data will be presented.

II. THE BMA BEAM DUMP

The **b**io**m**edical **a**rea (BMA) was located on the western edge of the PSI West accelerator facility - see Figure 1. One facility located in this area was the so called PIOTRON which was used to treat cancer patients with π^-. From the main beam a fraction of 20 μA could be split off with an electrostatic splitter. This fraction was

bent by two 45º dipole magnets onto the pion production target of the PIOTRON.

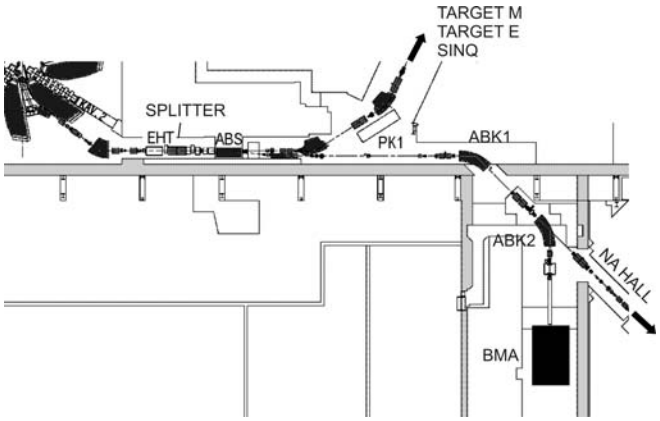

Figure 1: Schematic drawing of the beam line from the main ring cyclotron to the BMA area (black box). 20 μA of the 590 MeV proton beam could be split off and could be guided onto the pion production target of the BMA facility via the dipole magnets ABK1 and ABK2.

After passing through a last collimator the 590 MeV proton beam hit the helium cooled pion production target. The target was of cylindrical shape with a radius of 3 mm and a length of approximately 70 mm and was made from beryllium. The pions which emerged from the target under an angle of 60º with respect to the incident proton beam were bent by superconducting magnets to pass a huge shielding structure and after a distance of roughly 5 meters they were deflected onto the patients.

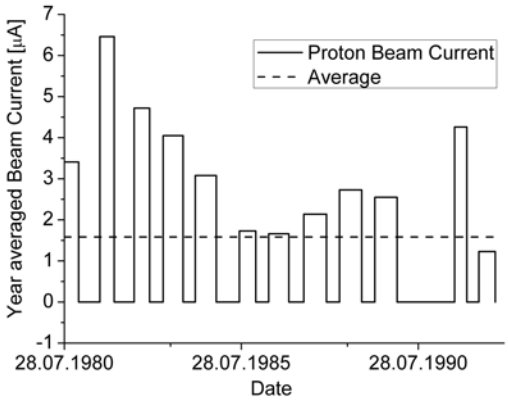

Figure 2: Proton current averaged over a run period as a function of time (solid line). The dashed line represents the average proton current over the lifetime of the PIOTRON.

The beam dump of the PIOTRON was located 40 cm behind the beryllium target. It was a water cooled copper block with a diameter of 8 cm and a length of 37 cm. The beam dump was surrounded by massive steel shielding. The PIOTRON in the BMA area started operation in 1980 and was shut down in September 1992. The operational cycle of the facility, extracted from Ref. 11, is given in Figure 2.

In 1992 dismantling started. The beam dump of the facility was shipped to the hot cell of PSI East where it was stored to cool down. In 1996 dose rate measurements were performed yielding dose rates of 300 mSv/h at 3 cm, 60 mSv/h in 30 cm and 10 mSv/h in 100 cm distance. In a first measurement campaign in 1999 the activities of several gamma emitting radioisotopes were measured; these results will not be presented here.

The beam dump was cut into 7 pieces of different lengths in the hot cell on the east side of PSI; the second piece is shown in Figure 3

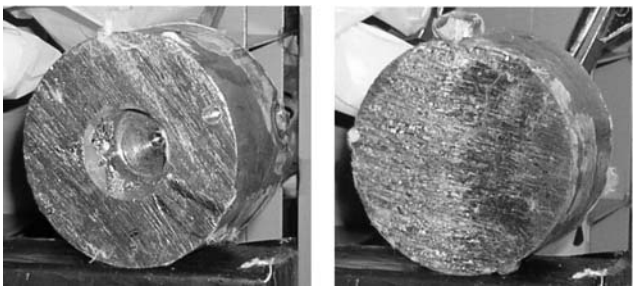

Figure 3: Photograph of the second beam dump piece of the BMA beam dump after cutting.

Samples were taken from each of those pieces by drilling on the beam entrance side. One sample each was taken from the copper block center and the second specimen position was located at the margin of each piece. For two beam dump sections a full radial sample profile was produced by drilling holes, radially separated by about 10 mm, starting at the center.

The content of isotopes of interest was then measured by different methods, dependent on the decay mode of the nuclide. Conventional γ-measurements with HPGe detectors were performed for ^{60}Co. For ^{108m}Ag a chemical separation prior to measurements was done to reduce the γ "background". The procedure for the separation is described in detail in Ref. 14. β-emitters like ^{63}Ni were measured by liquid scintillation counting (LSC) after a chemical separation from the bulk material. Accelerator mass spectrometry (AMS) was used at ETHZ/PSI Zurich[15] (Switzerland) and at Technical University of Munich[16] (Germany) to investigate the activities of the long-lived isotopes ^{26}Al, ^{36}Cl, ^{44}Ti, ^{53}Mn, and ^{55}Fe.

III. THE ACTIVATION CALCULATION

The activation calculations have been performed with a patched version of MCNPX 2.5.0[12] and the newly developed activation script as a driver for the activation calculation with SP-FISPACT[6]. SP-FISPACT is a modified version of FISPACT[6]; residuals produced by

high energy particles can be treated besides the activation of neutrons below 20 MeV. High energy in this context means reactions in which physics models are used to evaluate the products rather than tabulated cross section data. The version of SP-FISPACT was further extended to allow for high energy gas production as well (for tritium production this is essential). A scheme of the activation calculation is shown in Figure 4. The patched version of MCNPX 2.5.0 allows producing residual nuclei data directly, without the intermediate storage of this information on the histp file. Therefore, the use of the HTAPE3X program is obsolete which speeds up the calculation and reduces the size of files to be handled.

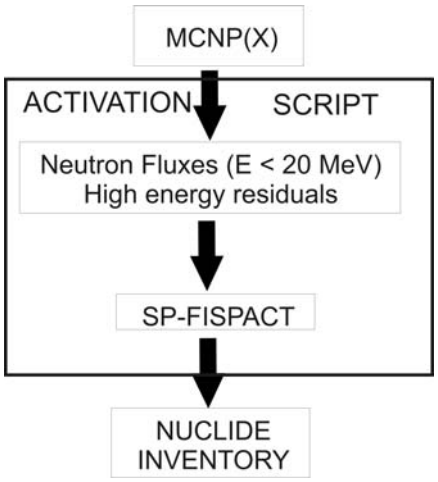

Figure 4: Scheme of the activation calculation. MCNPX is used to evaluate the neutron fluxes with energies below 20 MeV and residual nuclei from the physics model region. This information is passed into SP-FISPACT together with an irradiation history by the activation script, yielding a nuclide inventory at a given time.

The geometry used for the calculation is shown in Figure 5. The beam dump is modeled with longitudinal and radial segments. Overall it consists of 98 individual cells to account for the different sample locations. The pion production target is modeled as pure beryllium with a density of 1.70 g/cm^3. The beam dump is situated in a massive steel shielding block. The low energy neutron fluxes are provided in the VITAMIN-J format which is supported by (SP-) FISPACT. For the activation calculation with (SP-) FISPACT the EAF-2003 activation cross sections[13] have been used.

MCNPX calculations were performed with three different models; the Bertini INC event generator together with the Dresners evaporation model (BERTINI), the CEM2K model (CEM) and the intranuclear cascade model from Liege with the ABLA evaporation model (INCL).

There are several sources of uncertainty for the calculation; no information about the proton beam profile on the beryllium target could be found. Therefore, a pencil beam was modeled. In order to study the influence of the beam profile calculations were performed with a beam of gaussian shape with σ=3mm. The results with the 3mm beam only differ in very first central cell by approximately 10% from the predictions when a pencil beam is used. Furthermore, the composition of materials used in the PIOTRON is not known; trace elements and impurities of the beam dump material were not recorded. However, from the design drawings it is known that the beam dump was fabricated from OFHC copper. In the calculation an averaged OFHC copper composition is used, see Table 1. This averaged composition was obtained from the analysis of several copper samples at PSI.

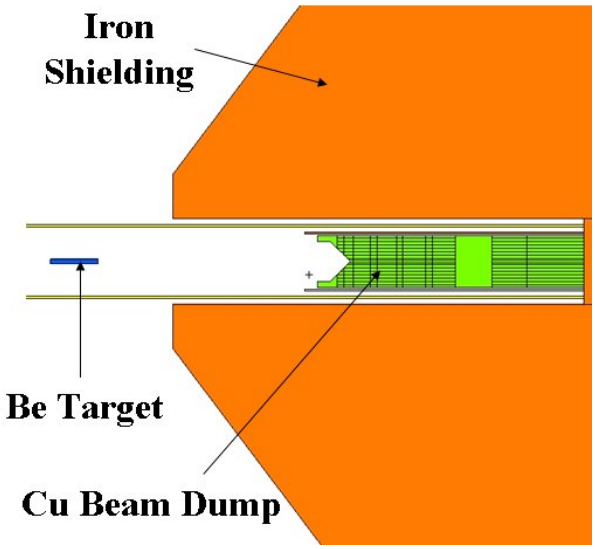

Figure 5:MCNPX geometry of the BMA beam dump. Protons come from the left. They hit the cylindrical beryllium target and are stopped in the beam dump. The surrounding steel shielding is depicted as well.

The irradiation history, as depicted in Figure 2, was simplified by assuming a continuous irradiation of the BMA beam dump for 12.2 years with 1.58 μA of 590 MeV protons. The effect of this simplification was investigated by comparing results of the calculation with the "correct" irradiation sequence and the simplified is on the order of 10% for most of the isotopes, for ^{110m}Ag and ^{57}Co it is about 30%.

IV.RESULTS

In Figure 6 a zoom into the front-end region of the beam dump is shown. As explained in the previous chapter the beam dump was cut into seven pieces and samples were taken by drilling. The sample positions were located in the longitudinal segments indicated with the arrows in Figure 6. A rather fine radial separation into

8 pieces was realized in the simulation, starting with a radius of 2.5 mm, 5 mm and then continuing in 5 mm steps.

Table 1: Composition of the copper used in the MCNPX calculation. A density of ρ =8.96 g/cm^3 was used.

Element	wt ppm	Element	wt ppm
Cu	999769.0	Na	1.0
Fe	60.0	Cr	1.0
P	40.0	Cs	1.0
Cl	30.0	Ho	1.0
S	15.0	Si	1.0
Ag	13.0	As	1.0
N	10.0	Rb	1.0
Al	10.0	Bi	1.0
Pb	8.0	Mn	0.5
Zn	6.0	Mg	0.5
Sn	5.0	Co	0.5
Ni	4.0	Li	0.5
Mo	3.0	B	0.5
Ca	2.5	K	0.5
Ga	2.0	Th	0.5
Hg	2.0	U	0.5
V	1.5	Ba	0.4
Ti	1.0	Eu	0.2

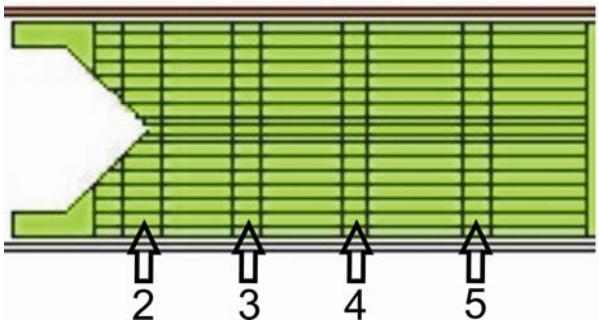

Figure 6: Detailed view of the MCNPX model of the BMA beam dump. The cutting positions (arrows) and drillings have been modeled by subdividing the copper into individual cells.

As the positioning for drilling probes from the beam dump had to be done remotely, the experimental data possess an error of 2 mm in position. In addition the drill holes have a diameter of 5-6 mm. Therefore, the total error in position for the experimental data was estimated to be 5 mm.

If it is not otherwise indicated, the specific activities refer to January 2006.

IV.A. ^{108m}Ag

The first radionuclide analyzed was ^{108m}Ag. The results of MC calculations with the three different intranuclear cascade models and the experimental specific activities (on January 1st 2000) for the samples from piece 3 are plotted in Figure 8. One can see a decrease of activity from the center of the beam dump to its edge, which is caused by the fall-off of high energy fluxes from the beam dump center to the outer regions of the beam dump. This is further explained in the following paragraph.

The ^{108m}Ag is produced from a Ag impurity in the copper, 13 weight ppm in the simulation (see Table 1), by the reactions ^{107}Ag(n,γ)^{108m}Ag and ^{109}Ag(n,2n)^{108m}Ag. In Figure 7 the one-group cross sections - as defined in Eq. (1) - for the two reactions calculated with SP-FISPACT are depicted as a function of the beam dump radius.

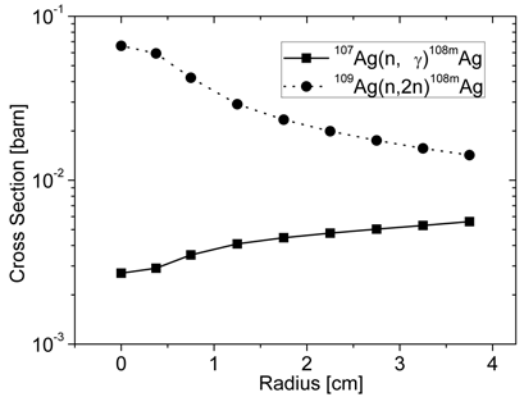

Figure 7: One-group cross sections for ^{107}Ag(n,γ)^{108m}Ag and ^{109}Ag(n,2n)^{108m}Ag as a function of the beam dump radius.

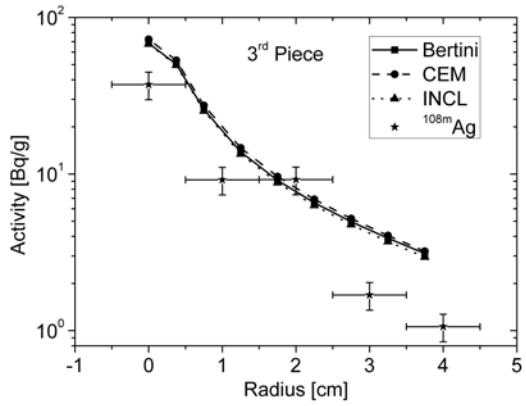

Figure 8: Radial distribution of specific activities of ^{108m}Ag in the third piece of the beam dump. The solid line is obtained by simulations with BERTINI together with the Dresner evaporation model, the dashed line was produced with CEM2K and INCL/ABLA results are represented by the dotted line. Experimental data are represented by stars.

Figure 7 indicates that the production of ^{108m}Ag is dominated by the (n,2n) reaction on ^{109}Ag. This reaction has a threshold of approximately 9 MeV. As high energy reactions, i.e. reactions in the physics model region, on the silver will hardly be modeled due to their extremely low probability the calculated activity is caused by neutrons with energy below 20 MeV. Hence, the production of ^{108m}Ag in the simulations is mainly caused by neutrons below 20 MeV and above 9 MeV in the beam dump center. At the rim there is a 2.5:1 ratio for (n,2n) over the (n,γ) reaction. From this the fall-off of the specific activity from the center to the edge of the beam dump can be explained by the decrease of the neutron flux between 9 and 20 MeV.

$$\sigma_1 = \frac{\int_{E=0MeV}^{E=20MeV} \Phi(E)\sigma(E)dE}{\int_{E=0MeV}^{E=20MeV} \Phi(E)dE}. \qquad (1)$$

As the neutron spectra of the three models are similar in the energy range from 9-20 MeV hardly any differences are found among the theoretical predictions; they agree within 10%.

The theoretical data overestimate the silver production. In the center this is to some extent caused by the pencil beam definition in the calculation. However, the influence is on the 10 % level. The slope of theoretical predictions does reproduce the strong decrease seen from the samples. A reduction of the silver content in the assumed copper composition by a factor of 2 would lead to an excellent agreement between theoretical and experimental data.

IV.B. ^{26}Al

All isotopes that have been investigated are mainly produced in high energy reactions. The high energy fluxes decline with increasing radius. As a consequence the activity distributions exhibit a decrease towards the rim of the beam dump. For ^{26}Al - the reaction with the highest Q value (~ 350 MeV) - the results are depicted in Figure 9. The main reaction channel is Cu(n,spall)^{26}Al, followed by the (n,2n) reaction on the Aluminum impurity.

INCL and CEM model this deeply inelastic collision slightly better than BERTINI does. The fall-off of calculated activities to a value of about 2 10^{-3} Bq/g reflects the high energy nature of this reaction. The activity on the 10^{-3} Bq/g level is caused by low energy neutron activation on the 10 ppm aluminum impurity present in the copper. The spikes at the different radii indicate high energy events with low statistics; Convergence has not been achieved here.

The experimentally observed ^{26}Al concentrations in the center of the copper section are under predicted by the calculations by at least an order of magnitude. For the rim no statement can be made due to the low statistics. However, the underestimation in the central part indicates the deeply inelastic collisions are not properly modeled by the combination of intranuclear cascade and evaporation codes.

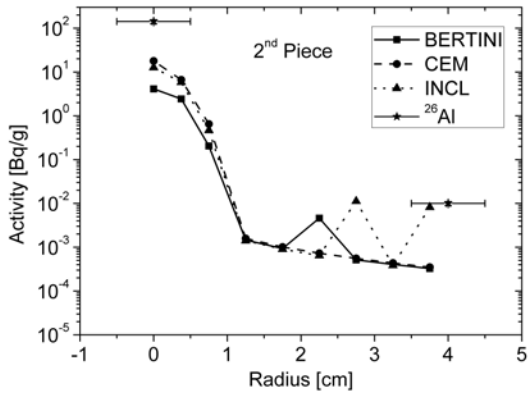

Figure 9: Specific activities of ^{26}Al as a function of radius in the beam dump. INCL (dotted) and CEM (dashed) modeled this deeply inelastic reaction slightly better than BERTINI (solid line). Experimental data are represented by stars; the errors of the activity are of the size of the symbols. The spikes at larger radii are explained in the text.

IV.C. ^{36}Cl

For chlorine only few data points have been measured by AMS so far, so that a conclusive statement about the experimental activity distribution can not be made. The main production channels are the direct production from Cu by spallation, ^{35}Cl(n,γ)^{36}Cl and ^{37}Cl(n,2n)^{36}Cl.

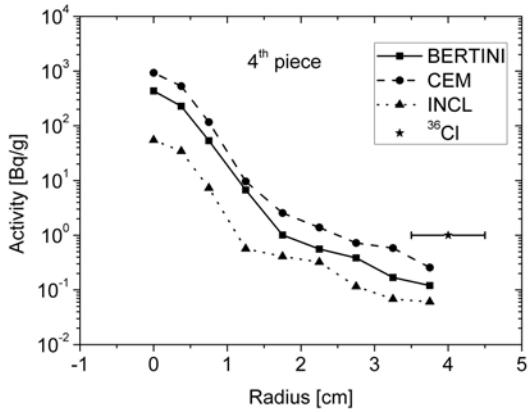

Figure 10: Radial distribution of the activity of ^{36}Cl in the 4th piece of the BMA beam dump. CEM (dashed line) gives the highest activities. INCL (dotted line) shows the

lowest activities and BERTINI (solid line) lies in between the two. The experimental value is represented by a star.

Theoretical predictions provide a similar trend of ^{36}Cl activities as in the aluminum case. However, the statistics is better due to less energy transfer needed for the production. All theoretical predictions exhibit the fall-off with increasing radius. CEM tends to give the highest specific activities and therefore lies closer to the measured data point. INCL gives the lowest activities and BERTINI results lie in between. Among themselves the theoretical predictions show differences of more than an order of magnitude in the central region.

IV.D. ^{44}Ti

The production of ^{44}Ti can be regarded as a one step process, if the fast decay from the possible ancestors ^{44}V ($\tau_{1/2}$=104 ms) and ^{44}Cr ($\tau_{1/2}$=53 ms) is disregarded. Assuming the composition given in Table 1 to be correct, it will be produced in large amounts by spallation on copper only. Therefore, the decay towards the outer region of the beam dump is observed once more in the experimental data - see Figure 11.

With decreasing Q-values the differences of theoretical predictions among themselves decrease. For ^{44}Ti INCL gives results higher by a factor of roughly 2.5 compared to CEM and BERTINI. As an example the radial distribution of ^{44}Ti in the third piece of the beam dump is shown in Figure 11. The over prediction of activities in the center is again visible. Nevertheless the shape of the radial distribution of activity of ^{44}Ti is well reproduced by all models.

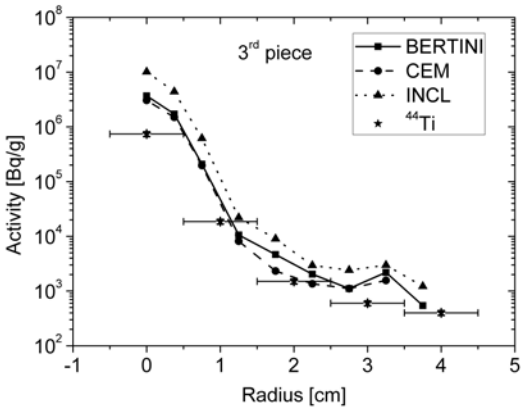

Figure 11: Radial distribution of ^{44}Ti in the third piece of the beam dump.

IV.E. ^{53}Mn

Three possible production channels for ^{53}Mn have been identified: ^{55}Mn(n,3n)^{53}Mn, ^{54}Fe(n,d)^{53}Mn, Cu(x,spall)^{53}Mn. Although the one-group cross section of ^{54}Fe(n,d)^{53}Mn is in the order of 15 mb the dominant reactionis the production from Cu with ~105 mb. The experimental data again exhibit the signature of high energy reactions - see Figure 12.

BERTINI and INCL data agree within 15% while CEM shows values which are 30% higher than BERTINI. For the central position experiment and theory match very well. No over prediction as in the other cases (except ^{26}Al and ^{36}Cl) is found for ^{53}Mn. For the outer measurement position a factor of 2 is observed between theoretical data and measurement. The general trend of the experimental results is reproduced by the calculations.

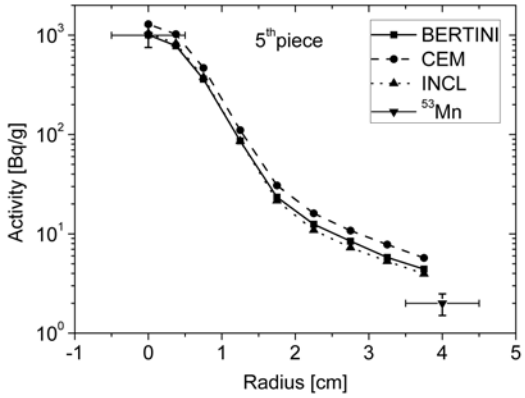

Figure 12: Specific activities of ^{53}Mn for the beam dump piece 5 calculated with the three models BERTINI (solid line), CEM (dashed line) and INCL (dotted line) as well as experimental data (stars).

IV.F. ^{55}Fe

For ^{55}Fe the spallation cross section is approximately an order of magnitude higher than the cross sections for neutron reactions below 20 MeV. The experimental data for the third beam dump section are displayed together with the theoretical predictions in Figure 13.

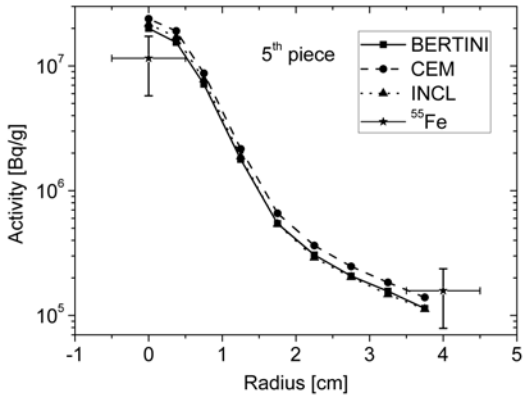

Figure 13: Radial distribution of ^{55}Fe in the third piece of the beam dump

The modeled data agree well with the experimental observations.

CEM and INCL predict higher concentrations for ^{55}Fe in the center than BERTINI. However, they agree within 20 %

IV.G. ^{60}Co

For ^{60}Co the activities for the beam dump piece 5 are given in Figure 1

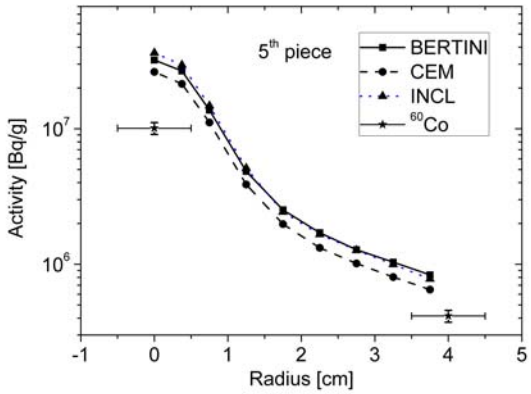

Figure 14: Specific activities of ^{60}Co for the beam dump piece 5 calculated with the three models BERTINI (solid line), CEM (dashed line) and INCL (dotted line) as well as experimental data (stars).

The overestimation in the center is found to be around a factor of 3. At the edge of the beam dump the ratio to the experimental value drops to 2. The best fit to the data is found for CEM.

The predictions of the three models agree within 25%, with CEM giving slightly lower values than INCL and BERTINI.

IV.H. ^{63}Ni

Finally we present the theoretical and experimental data for ^{63}Ni for the beam dump pieces 2, 4 and 5- see Figure 15 -17.

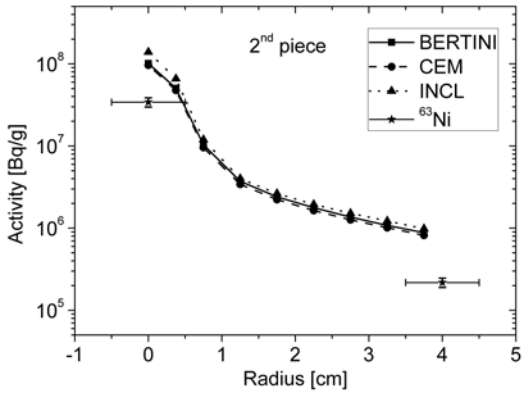

Figure 15: Specific activities for ^{63}Ni for the beam dump piece 2.

In all cases there is a clear overestimation of theory with respect to the experimental data (factor 2 - 4).

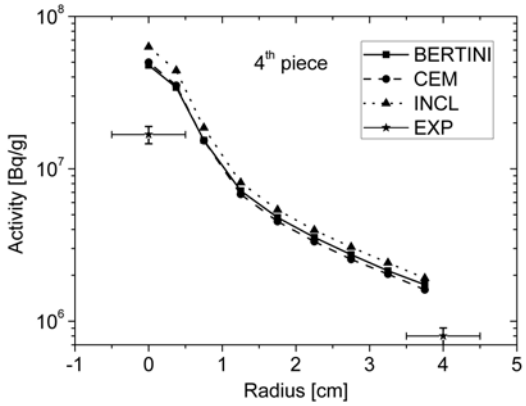

Figure 16: Same as Figure 15 but for piece 4.

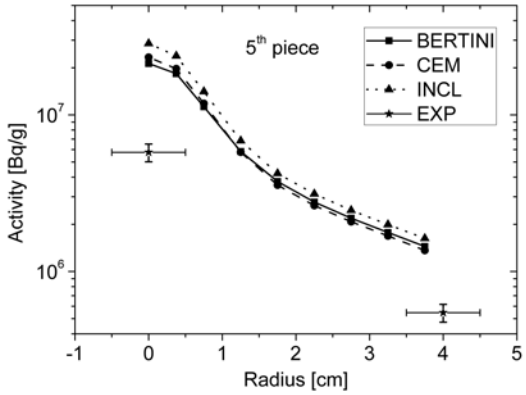

Figure 17: Same as Figure 15 but for piece 5.

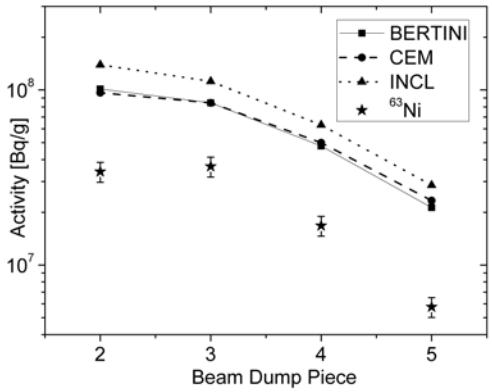

Figure 18: Longitudinal distribution of ^{63}Ni in the beam dump.

The longitudinal distribution of activity of ^{63}Ni in the beam dump is depicted in Figure 18.

The slope of the decrease of activity along the beam dump axis is steeper for experimental values than for data obtained by calculations.

Predictions of CEM and BERTINI agree within 7 % while INCL shows 30 % higher production rates in the center of the beam dump. Towards the rim a the differences decrease to the 10 % level.

V. SUMMARY AND OUTLOOK

A validation of MCNPX in conjunction with the buildup and decay code SP-FISPACT based on specific activities of long-lived radionuclides extracted from a copper beam dump has been performed. The agreement between experimental and theoretical data varies from a factor of 10 for deeply inelastic reaction down to a factor of 2 for reactions leading to nuclides not far from the parent isotope.

For high Q-value reaction, Al and Cl, models underpredict the specfic activities by an order of magnitude. For Ti a good description of the shape of experimental values is found, whereas the central activity is clearly overestimated. For ^{53}Mn and ^{55}Fe the description by the models is well. For lower Q-values an overestimation by BERTINI, INCL and CEM are found.

Between the various physics models implemented in MCNPX differences were observed for deeply inelastic reactions. A statement on the magnitude can not be given here, as convergence was not achieved in the calculations for the outer regions of the beam dump. For reaction products close to the parent nuclide differences on a 30% level are found.

It was already stated that not all nuclides have been successfully measured for all sample positions. It is however planned that as soon as all data have been acquired the whole set will be published.

ACKNOWLEDGMENTS

We would like to thank Sabine Teichmann for fruitful discussions and steady support.

REFERENCES

1. D. Pelowitz, ed., *MCNPX User's Manual, Version 2.5.0*, LA-CP-05-0369 (2005).
2. http://www.fluka.org/
3. Gallmeier et al., Proc. of the Eighth Int'l Topical Meeting on Nuclear Applications and Utilization of Accelerators, Pocatello, ID (2007).
4. X-5 Monte Carlo Team, "MCNP – A General Monte Carlo N-Particle Transport Code, Version 5," LA-UR-03-1987 (2003).
5. W. B. Wilson et al., "Recent Developments of the CINDER'90 Transmutation Code and Data Library for Actinide Transmutation Studies," Proc. GLOBAL'95 Int. Conf. on Evaluation of Emerging Nuclear Fuel Cycle Systems, Versailles, France (1995).
6. R.A. Forrest, *FISPACT-2003: User manual*, UKAEA FUS 485, (2002).
   C. Petrovich, *SP-FISPACT2001 A computer code for activation and decay calculations for intermediate energies. A connection of FISPACT to MCNPX.*, RT/ERG/2001/10, ENEA Bologna (2001)
7. F. Atchison and H. Schaal, *ORIHET3 - Version 1.12 A guide for users* , private communication (2001).
8. M. Brugger, H. Khater, S. Mayer, A. Rpinz, S. Roesler, L. Ulrici and H. Vincke, *Benchmark Studies of induced radioacivity produced in LHC materials, part I: specific activities*, Rad. Prot. Dosimetry 116, 6, (2005).
9. Y. Titarenko et al, *Experimental and theortical study of yields of residual product nuclei in thin targets irradiated by 100 - 2600 MeV protons*, IAEA, Nuclear Data Section, INDC(CCP)-434, (2002), available online via:
   http://www-nds.iaea.org/reports/indc-ccp-434.pdf.
10. L. Ulrici, M. Brugger, Th. Otto and S. Roesler, *Radionuclide characterization studies of radioactive waste produced at high-energy accelerators*, Nucl. Instr. Meth. in Phys. Res A 562, 596 (2006).
11. F. Atchison, A.C. Mezger, P. A. Schmelzbach, *Operations data for the PSI accelerators and user areas over the period 1974 to 2003, for use with the PWWMBS system*, TM-85-04-07 (2004).
12. F. Gallmeier, private communications (2007).
13. R. A. Forrest, J Kopecky and J-Ch Sublet, *The European Activation File: EAF-2003 cross section library*, UKAEA FUS 486, (2002).
14. D. Schumann; R. Michel, G. Korschinek, K. Knie, J.-Ch. David, *Excitation functions for the production of*

^{60}Fe and ^{53}Mn in the reaction ^{nat}Pb(p,xp/yn)Z, Nucl. Instr. Meth. in Phys. Res A 562, p. 1057 (2006).
D. Schumann, R. Weinreich, R. Michel, H.-A. Synal, P. Kubik, in the proceedings of International Conference on Nuclear Data for Science and Technology, Santa Fe, 2004, AIP Conference Proceedings Vol.769, p. 1517
D. Schumann, J. Neuhausen, R. Weinreich, F. Atchison, P.W. Kubik, H._A- Synal, G. Korschinek, T. Feastermann, submitted to Nucl. Instr. Meth. in Phys. Res B 2007
15. H.-A. Synal, G. Bonani, M. Döbeli, R. M. Ender, P. Gartenmann, P. W. Kubik, Ch. Schnabel, M. Suter, *Status report of the PSI/ETH AMS facility*, Nucl. Instr. and Meth. in Phys. Res B 123, p.62 (1997).
16. K. Knie, T. Faestermann, G. Korschinek, G. Rugel, W. Rühm, C.Wallner, *High-sensitivity AMS for heavy nuclides at the Munich Tandem accelerator*, Nucl. Instr. and Meth. in Phys. Res B 172, p. 717 (2000).